OPEN ACCESS
11th International Conference on New Frontiers in Physics
(ICNFP 2021)
International Journal of Modern Physics: Conference Series
Vol. 51 (2023) 2361006 (13 pages)

DOI: 10.1142/S2010194523610062

Rare nuclear processes in Hf isotopes

V. Caracciolo*, P. Belli, R. Bernabei, R. Cerulli, A. Leoncini and V. Merlo

Dipartimento di Fisica, Università di Roma "Tor Vergata", I-00133, Rome, Italy
INFN sezione Roma "Tor Vergata", I-00133 Rome, Italy
**vincenzo.caracciolo@roma2.infn.it*

F. Cappella and A. Incicchitti

Dipartimento di Fisica, Università di Roma "La Sapienza", I-00185, Rome, Italy
INFN sezione Roma, I-00185 Rome, Italy

M. Laubenstein and S. Nisi

INFN, Laboratori Nazionali del Gran Sasso, I-67100 Assergi (AQ), Italy

S. S. Nagorny

Arthur B. McDonald Canadian Astroparticle Physics Research Institute;
Department of Physics, Engineering Physics and Astronomy,
Queen's University, K7L 3N6 Kingston, Canada

P. Wang

Department of Chemistry, Queen's University, ON K7L 3N6, Kingston, Canada

Published 27 December 2023

Recently, efforts on the building of Hf-based crystal scintillators have been performed. The so-called "source = detector" approach has been implemented to study rare nuclear processes in Hf isotopes with higher efficiency with respect to the HP-Ge spectrometry. In this work, a review of recent studies concerning rare nuclear processes in Hf isotopes are presented.

1. Introduction

A fascinating topic of nuclear physics is the nuclear instability, which plays an important role in nuclear models, electroweak interaction, and conservation laws.

Here, the current status of the experimental searches for rare α and double beta decay (DBD) in Hf-isotopes is reviewed.

The DBD is a significant nuclear decay for neutrino physics, to test, e.g., the calculations of different nuclear shapes and the decay modes that involve the vector and axial-vector weak effective coupling constants (g_A), etc. The DBD without neutrinos emission is a process requiring lepton-number violation, in addition to a non-vanishing neutrino mass that requires a Majorana mass component. Therefore, it could be often regarded as the golden-standard process for probing the fundamental nature of neutrinos. The DBD is a higher-order effect with respect to the β-decay: the expected half-lives are longer than those of the β-decay, and roughly of the order of 10^{20} y. Therefore, special experimental care has to be taken to study this process. Thus, the 0νDBD is of great interest because, if observed, it can open a new window beyond the Standard Model (SM). The number of candidates isotope to this study are 69, in particular, 35 via the emission of two e^- and 34 in positive channels: either two positron emission ($2\beta^+$) or a positron emission with an electron capture ($\epsilon\beta^+$) or a double electron capture (2ϵ)[1–3]. The simultaneous study of positive and negative DBD can constrain the theoretical parameters with very high confidence, giving mutual information. Moreover the nuclear matrix elements for the two-neutrino mode and the neutrinoless mode can be related to each other through relevant parameters: in the free nucleon interaction, the g_A value is 1.2701, but, when considering a nuclear decay, there are indications that the phenomenological axial-vector coupling value is reduced at $g_A < 1$, more precisely: $g_A \sim 1.269A^{-0.18}$ or $g_A \sim 1.269A^{-0.12}$, depending on the nuclear model adopted to infer the g_A value.[1] Thus, DBD investigation with various nuclei would shed new light on constraining these and other important model-dependent parameters. In addition, in case of the $0\nu2\epsilon$ mode, it is possible to study also the so-called "resonant effect".[1,2]

Besides these, various theoretical models are continuously developed or improved, motivated, for example, by searches for stable or long-lived superheavy isotopes and predictions of their half-lives. The study of rare α decay plays an important role in the foundation and development of nuclear physics. It can offer information about the nuclear structure, nuclear levels, and nuclear properties. Furthermore, the phenomenon of α decay can provide information about the fusion-fission reactions since the α decay process involves sub-barrier penetration caused by the interaction between the α and the nucleus.[4] In addition, as a byproduct, such researches contribute to develop new detectors and perform news protocols to purify materials containing DBD or rare α emitters from radio-impurities.[5–22]

2. Searching for Double Beta Decay in Hafnium Isotopes

The ^{174}Hf isotope is a potentially DBD emitter via $\epsilon\beta^+$ and 2ϵ modes with a energy decay $Q_{2\beta} = 1100.0(23)$ keV[23] and an isotopic abundance $\delta = 0.156(6)\%$.[24] A simplified $\epsilon\beta^+$ and 2ϵ decay scheme of ^{174}Hf is shown in Fig. 1. The theoretical

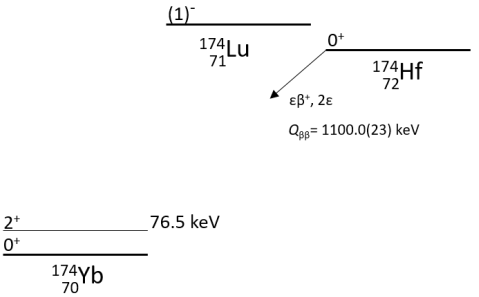

Fig. 1. Simplified $\epsilon\beta^+$ and 2ϵ decay scheme of ^{174}Hf.

half-life estimations of the $\epsilon\beta^+$ and 2ϵ of ^{174}Hf are not present in literature (to our knowledge) but the values of the phase space factor involved are $(0.001-7.5)\times10^{-30}$ y^{-1}, $(0.003-1)\times10^{-17}$ y^{-1} respectively for the $2\nu\epsilon\beta^+$ and $0\nu\epsilon\beta^+$ transitions[25] and $(1.6-3.5)\times10^{-21}$ y^{-1} for the $2\nu2\epsilon$ transition.[25] Considering that typically the magnitude of the nuclear matrix element of the 2νDBD is of the order of $1-10$, the half-life estimations are roughly $10^{28}-10^{33}$ y and $(0.3-6)\times10^{19}$ y respectively for the $2\nu\epsilon\beta^+$ and $2\nu2\epsilon$ transitions.

In 2020 and 2021 two independent experiments,[26,27] the first one performed at HADES laboratory of the Joint Research Centre of European Commission (Geel, Belgium) and the second one at the underground National Laboratory of Gran Sasso in Italy, searched for the 2ϵ and $\epsilon\beta^+$ decay of ^{147}Hf. In both cases, a passive approach, using a gamma-ray spectrometry technique, has been adopted.

The experiment at HADES in Ref. 26 used a sample of metallic hafnium with sizes ⌀59.0 mm ×5.0 mm (total mass of 179.8 g that contained ∼ 0.29 g of the isotope ^{174}Hf). The experimental set-up was arranged in two different configurations, and the approach was to install the Hf-sample between the endcap of two HP-Ge detectors arranged back-to-back. The total exposure of the experiment was 42 g×d for the isotope ^{174}Hf. Instead, the experiment at LNGS in Ref. 27 used a foil of metallic hafnium of 55.379(1) g. The HP-Ge (⌀70 mm × 70 mm) was covered by the hafnium foil. In particular, the foil thickness (0.25(1) mm) was optimized to minimize the self-absorption of low-energy γ and X-rays within the sample itself and improve the overall detection efficiency. The data was collected over 310 d.

Considering the 2ϵ transitions of ^{174}Hf, in case of a $2K$ or KL capture in ^{174}Hf, a cascade of X-ray (and Auger electrons) of ^{170}Yb atom with energies in the range of $(50.8-61.3)$ keV is expected, while energies of the $2L$ capture X-ray quanta are $\simeq(7-10)$ keV, these latter were below the detectors' energy thresholds of both the experiments. Thank to these X-rays, the decay modes $2K$ and KL to the ground state (g.s.) of the ^{170}Yb have been studied by both experiments, besides the transition to the first excited level of the daughter nucleus.

In Refs. 26, 27, no peculiarity was observed ascribing to the DBD processes of ^{174}Hf; thus, in Table 1, the half-life limits have been reported.

Table 1. The half-life limits of 2ϵ and $\epsilon\beta^+$ processes in ^{174}Hf as performed in Refs. 26, 27.

Channel of the decay	Decay Mode	Level of daughter nucleus J^π, energy (keV)	Experimental limit of $T_{1/2}$ (90% C.L.) (y) [26]	[27]
$2K$	2ν	g.s.	$\geq 7.1 \times 10^{16}$	$\geq 1.4 \times 10^{16}$
KL	2ν	g.s.	$\geq 4.2 \times 10^{16}$	$\geq 1.4 \times 10^{16}$
$2K$	2ν	2^+, 76.5	$\geq 5.9 \times 10^{16}$	$\geq 7.9 \times 10^{16}$
KL	2ν	2^+, 76.5	$\geq 3.5 \times 10^{16}$	$\geq 7.9 \times 10^{16}$
$2L$	2ν	2^+, 76.5	$\geq 3.9 \times 10^{16}$	$\geq 7.9 \times 10^{16}$
$2K$	0ν	g.s.	$\geq 5.8 \times 10^{17}$	$\geq 2.7 \times 10^{18}$
KL	0ν	g.s.	$\geq 1.9 \times 10^{18}$	$\geq 4.2 \times 10^{17}$
$2L$	0ν	g.s.	$\geq 7.8 \times 10^{17}$	$\geq 3.6 \times 10^{17}$
$2K$	0ν	2^+, 76.5	$\geq 7.1 \times 10^{17}$	$\geq 2.4 \times 10^{18}$
KL	0ν	2^+, 76.5	$\geq 6.2 \times 10^{17}$	$\geq 3.1 \times 10^{17}$
$2L$	0ν	2^+, 76.5	$\geq 7.2 \times 10^{17}$	$\geq 9.4 \times 10^{17}$
$K\beta^+$	$2\nu + 0\nu$	g.s.	$\geq 1.4 \times 10^{17}$	$\geq 5.6 \times 10^{16}$
$L\beta^+$	$2\nu + 0\nu$	g.s.	$\geq 1.4 \times 10^{17}$	$\geq 5.6 \times 10^{16}$

3. Searching for Alpha Decays in Hafnium Isotopes

Natural hafnium consists of six isotopes; all of them are theoretically unstable concerning the α decay with a Q_α value in the range of $1.3 - 2.5$ MeV. The Hf isotopes with natural abundance and with $Q_\alpha > 0$ are listed in the Table 2. All of them can decay to g.s. or excited levels of their daughters. Figure 2 shows simplified decay schemes of the α decay of the naturally occurring Hf isotopes. In the decays of such Hf isotopes to excited levels, γ quanta are emitted. In this case, a searching using low-background γ spectrometry can be implemented. Moreover, considering the case of $^{179}\text{Hf} \rightarrow {}^{175}\text{Yb}$ decay, because the ^{175}Yb is unstable via β^- decay with $T_{1/2} = 4.185(1)$ d,[33] also the ^{179}Hf decay to the g.s. of daughter ^{175}Yb can be evaluated using the mentioned passive technique. Considering that approach and using HP-Ge detectors, two experimental set-ups were realized (see Refs. 28, 27). Besides these, an other interesting experiment, using an active approach, was performed in Ref. 24 to study some potentially α decay of Hf isotopes to g.s. or exited levels of daughter nuclei. The best obtained results are reported in Table 2 with the theoretical estimations.

In particular, Ref. 24 reports a direct study of the α decay of naturally occurring Hf isotopes by exploiting the "source=detector" approach with a Cs_2HfCl_6 crystal scintillator. There, after 2848 h of data taking, the α decay of ^{174}Hf was observed with $T_{1/2} = 7.0(1.2) \times 10^{16}$ y. The experiment was carried out at the STELLA facility of the LNGS. The Cs_2HfCl_6 (CHC) crystal scintillator with mass 6.90(1) g was coupled with a 3-inch low radioactivity photomultiplier (PMT, Hamamatsu

Table 2. Main potential α transition of Hf isotopes and related information. Only isotopes with natural abundance (δ) greater than zero (i.e. naturally present in nature) and with $Q_\alpha > 0$ between g.s. transitions or between g.s. and lowest bounded level transitions (with spin/parity J^π) are listed. Experimental measurements (if exist) and theoretical predictions on the half-lives are reported in the latest four columns.

Nuclide Transition	J^π Parent → Daughter Nuclei and its level (keV)	δ (%) [29]	Q_α (keV) [23]	$T_{1/2}$ (yr) Experimental	$T_{1/2}$ (yr) Theoretical [30]	[31]	[32]
^{174}Hf → ^{170}Yb	$0^+ \to 0^+$, g.s. $0^+ \to 2^+$, 84.2	0.156(6) [24]	2539(28)	$7.0(1.2) \times 10^{16}$ [24] $\geqslant 2.8 \cdot 10^{16}$ [27]	$3.5 \cdot 10^{16}$ $1.3 \cdot 10^{18}$	7.4×10^{16} 3.0×10^{18}	3.5×10^{16} 6.6×10^{17}
^{176}Hf → ^{172}Yb	$0^+ \to 0^+$, g.s. $0^+ \to 2^+$, 78.7	5.26(70)	2254.1(1.5)	$\geqslant 9.3 \times 10^{19}$ [24] $\geqslant 3.0 \times 10^{17}$ [28	2.5×10^{20} 1.3×10^{22}	6.6×10^{20} 3.5×10^{22}	2.0×10^{20} 4.9×10^{21}
^{177}Hf → ^{173}Yb	$7/2^- \to 5/2^-$, g.s. $7/2^- \to 7/2^-$, 78.6	18.60(16)	2245.6(1.4)	$\geqslant 3.2 \times 10^{20}$ [24] $\geqslant 1.3 \times 10^{18}$ [28]	4.5×10^{20} 9.1×10^{21}	5.2×10^{22} 1.2×10^{24}	4.4×10^{22} 3.6×10^{23}
^{178}Hf → ^{174}Yb	$0^+ \to 0^+$, g.s. $0^+ \to 2^+$, 76.5	27.28(28)	2084.2(1.4)	$\geqslant 5.8 \times 10^{19}$ [24] $\geqslant 1.3 \times 10^{18}$ [27]	3.4×10^{23} 2.4×10^{25}	1.1×10^{24} 8.1×10^{25}	2.2×10^{23} 7.1×10^{24}
^{179}Hf → ^{175}Yb	$9/2^+ \to 7/2^+$, g.s. $9/2^+ \to 9/2^+$, 104.5	13.62(11)	1807.6(1.4)	$\geqslant 2.5 \times 10^{20}$ [24] $\geqslant 2.7 \times 10^{18}$ [27]	4.5×10^{29} 2.0×10^{32}	4.0×10^{32} 2.5×10^{35}	4.7×10^{31} 2.2×10^{34}
^{180}Hf → ^{176}Yb	$0^+ \to 0^+$, g.s. $0^+ \to 2^+$, 82.1	35.08(33)	1286.9(1.4)	– $\geqslant 1.0 \times 10^{18}$ [28]	6.4×10^{45} 4.0×10^{49}	5.7×10^{46} 4.1×10^{50}	9.2×10^{44} 2.1×10^{48}

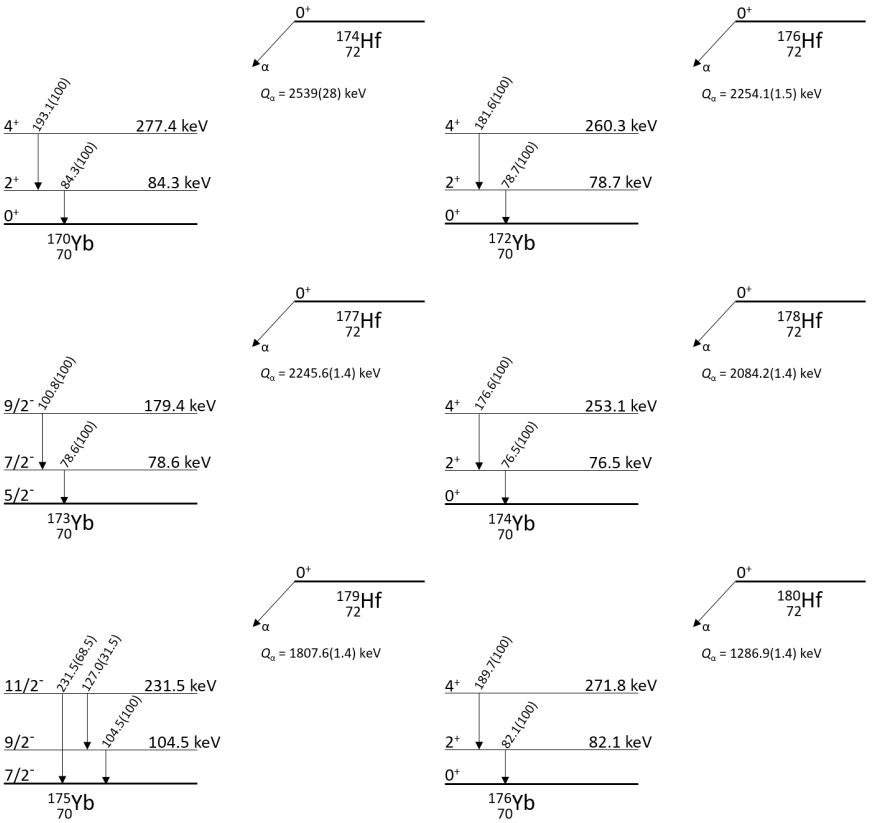

Fig. 2. Simplified decay schemes of potential α decay of Hf isotopes considering the first two energy levels of the daughter nuclei. The corresponding gamma transitions and the probability related for a single energy level are also shown. The ^{175}Yb isotope is unstable via β^- decay with $T_{1/2} = 4.185(1)$ d,[33] all the other Yb nuclei are stable.

R6233MOD), and placed above the end-cap of the ultra-low background HP-Ge γ spectrometer GeCris (465 cm^3). A schematic cross-section view of the experimental set-up is shown in Fig. 3.

The surface of the crystal was covered with a diffusive PTFE tape to improve the light collection. The CHC and HP-Ge detectors were installed inside a passive shield assembled (from the external to the internal part) with low radioactivity lead ($\sim$ 25 cm), with high purity copper ($\sim$ 5 cm), and, in the inner-most part, with archaeological Roman lead ($\sim$ 2.5 cm). The whole set-up – with the exception of the thermal contact with a metal rod called cold finger for the HP-Ge detector – was contained inside a plexiglas box and continuously flushed by high purity nitrogen gas to exclude the environmental air.

The signals from the PMT and the HP-Ge were acquired using a CAEN DT5720B digitizer operating at 250 MSamples/s; these signals were recorded in a

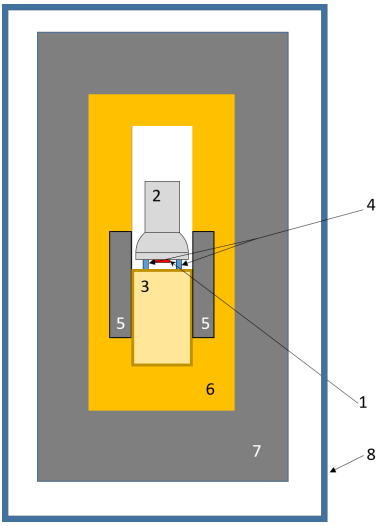

Fig. 3. Schematic cross-sectional view of the experimental set-up (not in scale). There are shown the CHC crystal scintillator (1) coupled with a 3 inches PMT (2), the HP-Ge detector (3), which is separated by a cylindrical teflon ring (4). They are completely surrounded by a passive shield made of archaeological Roman lead (5), high purity copper (6), low radioactive lead (7). The whole set-up (with the exception of the thermal contact of the HP-Ge crystal by a metal rod called "cold finger") is enclosed into a plexiglas box (8) continuously flushed with HP-N_2 gas (taken from Ref. 24).

time window of 50 μs. An event-by-event data acquisition system stored the pulse profiles of the events. The idea was to use a coincidence logic, between the CHC and the HP-Ge detectors, to study the α decay of Hf isotopes to the first excited level of the daughter nucleus, when a γ–ray of such a decay is emitted and can reach the HP-Ge detector.

The energy calibration and resolution of both CHC and HP-Ge detectors were determined by using calibration γ sources with peak energies 59.5 keV (^{241}Am), 511.0 keV (^{22}Na), 661.7 keV (^{137}Cs) and 1274.5 keV (^{22}Na)[a]. In particular, the energy resolution of the CHC detector depends according to the following formula: FWHM(keV) $= 0.53(5) \times E^{0.73(2)}$, where E is in keV. To monitor the stability of the energy scale, the data have been grouped in several runs and the stability in time of the energy spectra has been verified.

Moreover, a dedicated energy calibration of the CHC crystal scintillator by a ^{241}Am α source was performed in order to preliminarily estimate the quenching factor (Q.F.)[b] of the CHC. This source was placed in front of the CHC detector at a distance of about 1.5 cm.

[a]In the successive paragraphs, the spectra related to the CHC are in anticoincidence with the HP-Ge detector.

[b]The Q.F. describes the response of a scintillator to heavy ionizing particles; in details, it is the ratio between the detected energy in the energy scale measured with γ sources to the energy of

The PSD between β/γ and α particles, the so called Bi–Po events analysis, and the time-amplitude analysis of the fast sub-chains of α decays from the ^{232}Th family were applied in order to evaluate the radioactive contamination of the CHC crystal scintillator and the response of the detector to β/γ particles. In particular, the data of the radioactive contamination of the CHC crystal scintillator was used to build the background model to estimate the half-life of the α decays of Hf-isotopes.

The time profile of each event was exploited to calculate its mean time according to:

$$\langle t \rangle = \sum f(t_k) t_k \Big/ \sum f(t_k) \tag{1}$$

where the sum is over the time channels, k, starting from the origin of the pulse up to 8 μs. Moreover, $f(t)$ is the digitized amplitude (at the time t) of a given signal. The scatter plot of the mean time versus energy for the data of the low background

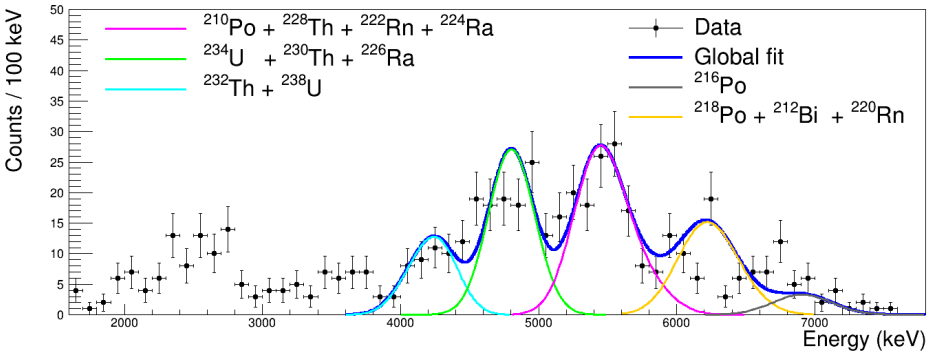

Fig. 4. Energy spectrum of the α events selected by PSD from the data of the low-background measurements with the CHC crystal scintillator over 2848 h. The fit of the data by the model built from α decays of ^{238}U and ^{232}Th with daughters is shown by blue solid line (individual components of the fit are shown too). The energy scale is in α energy having considered the Q.F. discussed in the text (see Ref. 24 for details).

measurements is shown in Fig. 5; it demonstrates the pulse-shape discrimination ability of the CHC detector. The distribution of the mean times for the events with energies – using the γ scale – in the range (0.4 – 3.0) MeV is shown in the inset of Fig. 5. The spectra of α events selected by PSD analysis are given in Fig. 4.

According to the result of the time–amplitude analysis, the Q.F. of the used CHC scintillator to α particles at the energies of ^{224}Ra, ^{220}Rn and ^{216}Po α decays was 0.39(4), 0.40(3), 0.40(3), respectively. Figure 6 shows these Q.F. values and the global fit (red dotted line) following the prescription of Ref. 35, showing that α particle produces about 1/2.5-th of the light produced by γ quanta in the energy

the heavy ionizing particle. The Q.F. is an experimental feature of a detector and it is strongly dependent on its nature, mechanisms of detection, impurities and so on.

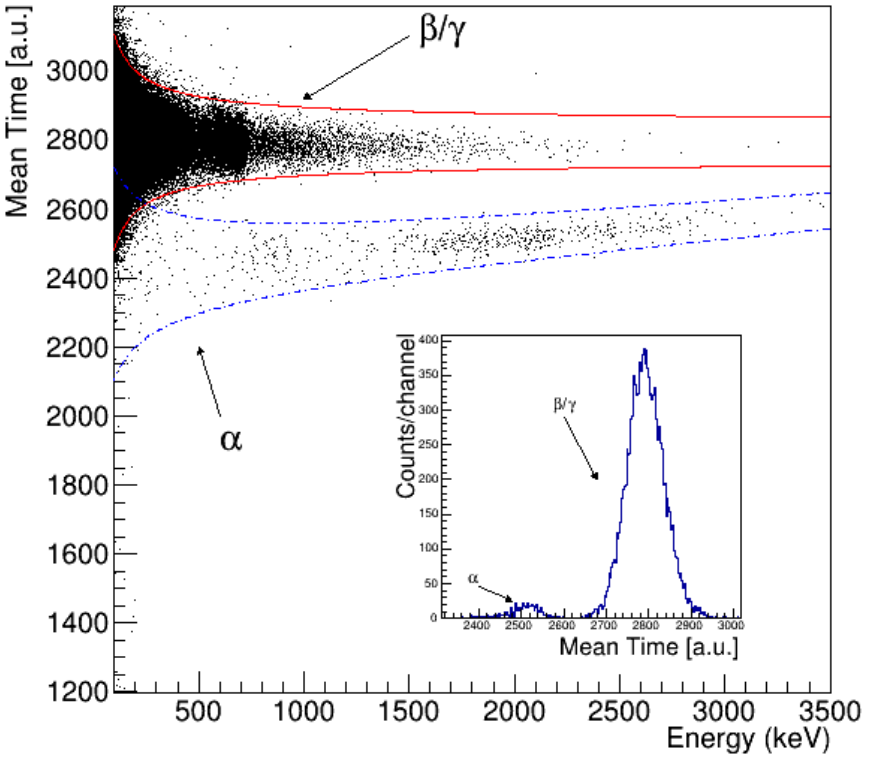

Fig. 5. Mean time (see text) versus energy for the low background data accumulated over 2848 h with the CHC detector. The x-sigma intervals, ($x = 2.57584$, consistent with the 99% of events), for the mean time values corresponding to β/γ and α particles are depicted (on-line: red solid lines and blue dashed lines, respectively). (Inset) Distribution of the mean times for the events with energies in the range of (0.4 – 3.0) MeV (taken from Ref. 24).

range (1–8) MeV[c]. For comparison, in Fig. 6 a linear fit (solid green line) of the same data is also shown. One can notice that the maximum Q.F. difference between the two models is ∼10%, in the energy range (1 – 8) MeV. However, considering the model of Ref. 35 the Q.F. at 4 MeV is in agreement with the Q.F. measured in Ref. 34. In the following, as reported in Ref. 24, the fit result according the model of Ref. 35 will be used.

The α spectrum was fitted by a model which accounts for the α peaks from ^{238}U, ^{232}Th and from their daughters, assuming broken equilibrium in the chains[d]. In Fig. 4 the energy scale is in α energy having considered the Q.F. model of Ref. 35 as discussed before (see Ref. 24 for details).

[c]Hereafter the energy is in α energy and not more in γ scale.
[d]The equilibrium can be broken in the chains because of the different chemical properties of the nuclides in U/Th chains and of the relatively large half-lives of some nuclides in the chains.

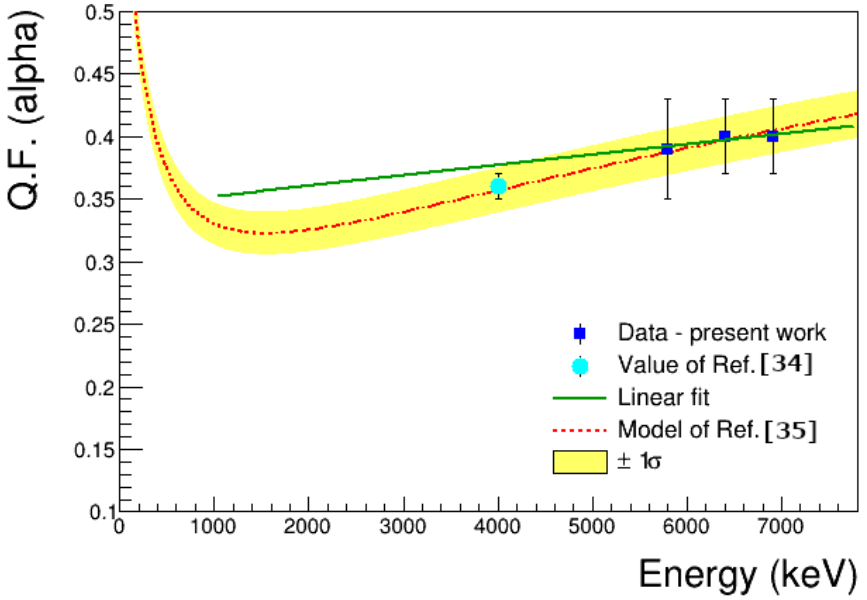

Fig. 6. Dependence of the Q.F. on the energy of the α particles measured by the internal α decays of ^{224}Ra, ^{220}Rn, ^{216}Po of the CHC crystal (blue squares). The model obtained as global fits of these data points following the prescription of Ref. 35 are also reported (red dotted line) with its 1σ fit uncertainty (yellow filled band). For comparison, a linear fit (solid green line) of the same data (blue points) is also shown. Moreover, the measured Q.F. for a CHC scintillator in Ref. 34 is also shown (cyan dot).

The α energy spectrum, above 4 MeV, was fitted using a model which includes the α peaks (see Ref. 24 for details) of ^{232}Th, ^{238}U and their daughters in order to study such contaminants. Besides this, such analysis was useful to have an additional check of the adopted Q.F. model. Later, we will focus the analysis in the energy range of interest to study the Hf α decays.

Considering all the α events, the total internal α activity in the CHC crystal is at the level of 7.8(3) mBq/kg.

When adopting the claimed half-life of the ^{174}Hf α decay of Ref. 36, the expected number of events in 2848 h of data taking with the CHC crystal (see Ref. 24 for details) is about 1100 counts. Thus, considering that all the measured α events was 553(23), even ascribing all of them to ^{174}Hf α decay (despite the analysis reported above), one can safely rule out the result given in Ref. 36; in fact, even in such an unlike hypothesis, the $T_{1/2}$ value derived in Ref. 24 would be $4.01(17) \times 10^{15}$ y, i.e. is about 4.5σ far from the value of Ref. 36: $T_{1/2} = 2.0(4) \times 10^{15}$. Thus, the $T_{1/2}$ value given in Ref. 36 was safely rejected. Let us now report a refined determination of the $T_{1/2}$ value of the ^{174}Hf α decay supported by the data in Ref. 24.

The background model in the energy interval (1.1 – 3.9) MeV, where the ^{174}Hf α decay is expected too, is made by an exponential function (to describe residual β/γ events), and suitable asymmetric Gaussian functions to describe the α decay

of ^{147}Sm (Q_α = 2311.2(10) keV), ^{174}Hf (Q_α = 2494.5(2.3) keV) and the events in the energy range (3.0-3.9) MeV (see Ref. 24 for details). These events were assumed as α degraded events from possible surface and other contamination. The FWHM of the peaks was bounded taking into account the dependence of the FWHM on energy for γ quanta as reported in before. For the case of asymmetric Gaussian used to model the α degraded events the left tail of the function was used as free parameter, instead the σ was limited by the FWHM energy dependence (see Ref. 24 for details).

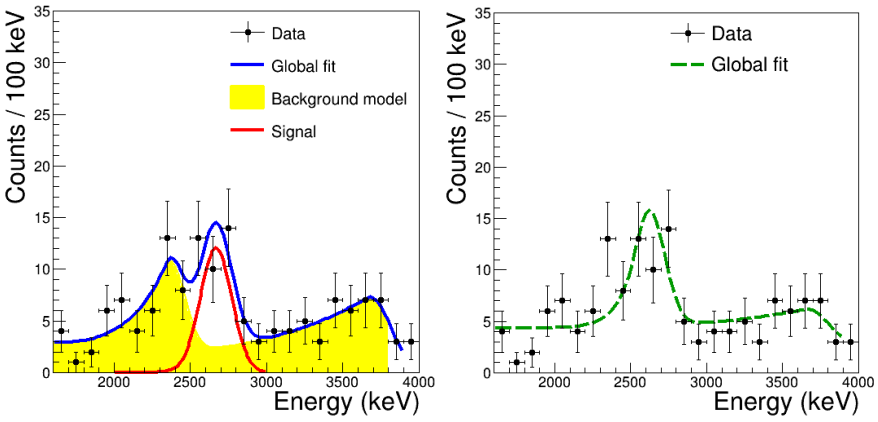

Fig. 7. Energy spectrum of α events selected by the pulse-shape discrimination from the data of low-background measurements with the CHC crystal scintillator over 2848 h. The energy scale is in α energy having considered the Q.F. (see text or Ref. 24 for details). (*left*) The fit of the data by the model built from α decays of the ^{174}Hf (red line) and of the ^{147}Sm plus degraded alpha particles is shown (blue solid line online). The yellow band is the background model with respect to the signal of the α decay of the ^{174}Hf nuclide. (*right*) The fit of the data by a modified model similar the previous one but considering just one peak (instead of two) in the energy (2.2–2.6) MeV (taken from Ref. 24).

The fit, in the range (1.1 – 3.9) MeV, provided the area of the peak searched for with $\chi^2/n.d.f.$=0.87 (P-value = 38.7%) and 31.7(5.6) events (see Fig. 7-left). The counts for the peak near 2.3 MeV are 29.5(5.4) in very good agreement with thus expected by data of ^{147}Sm reported in Table 7 of Ref. 24. The Q_α of ^{147}Sm and ^{174}Hf determined by the fit procedure show a slight variation of the mean value ($\sim$ 5%) in agreement with the uncertainty of the adopted Q.F. (see Ref. 24 for details) In addition to the χ^2 test, another independent statistical test was applied: the run test (see e.g. Ref. 37); it verified the hypothesis that the positive (above the fit value) and negative (under the fit value) data points were randomly distributed. The lower and upper tail probabilities obtained by the run test were 94% and 12% respectively.

The data in the range (2–3) MeV could be explained in principle by one single peak. In order to study this possibility a fit of same data as before was performed,

but considering only one peak in the energy (2 – 3) MeV instead of two (see Fig. 7-*right*); this fit yields a χ^2 probability of 1.7%.

To summarize, the analysis support that the data in Ref. 24 were statistically in good agreement with the assumed model, in particular with the assumptions of signals potentially due to the ^{147}Sm and ^{174}Hf α decays (first and second peak in Fig. 7-*left* respectively). To compute the half-life the following formula was used:

$$T_{1/2} = \ln 2 \cdot N \cdot \epsilon \cdot t \,/\mathrm{S}, \tag{2}$$

where N is the number of potentially α unstable nuclei ($N = 1.0 \times 10^{19}$), ϵ is the detection efficiency ($\epsilon = 99\%$, included the PSD efficiency), t is the measurements time, and S is the number of events of the effect searched for (31.7(5.6) events, see before). According to all this, the $T_{1/2}$ value for the α decay of ^{174}Hf is (see Ref. 24 for the extensive discussion about the data analysis and the relative uncertainties):

$$T_{1/2} = (7.0 \pm 1.2) \times 10^{16} \text{ y} \tag{3}$$

4. Conclusion

In this work, the experimental and theoretical studies concerning the rare decay of naturally occurred hafnium isotopes have been briefly reported. In particular, in Table 1 the half-life limits of 2ϵ and $\epsilon\beta^+$ processes in ^{174}Hf are shown. The half-life limits are at the level of $10^{16} - 10^{18}$ y. These values have to be compared to the values of the phase space factor predicted for such transition considering a nuclear matrix element of the order of 1-10 as typical for that calculations (see Sec. 2). Instead, in Table 2 the main potential α transition of Hf isotopes and the related experimental measurements and theoretical prediction of half-life are reported.

In particular, an experiment to study the α decay of naturally occurring hafnium to the ground state and the first excited state using a CHC crystal scintillator in coincidence with a HP-Ge detector was completed after 2848 h of live time (see Ref. 24). The analysis performed ruled out the $T_{1/2}$ value of α decay of ^{174}Hf nuclide given in Ref. 36. Furthermore, Ref. 24 was stated that the α decay of ^{174}Hf nuclide to the ground state was observed with a $T_{1/2} = 7.0(1.2) \times 10^{16}$ y. This value is in good agreement with the theoretical predictions reported in Table 2.

Besides this result, no decay was detected for α and double beta decay of ^{174}Hf, ^{176}Hf, ^{177}Hf, ^{178}Hf, ^{179}Hf, ^{180}Hf nuclides either to the ground state or to the lower excited levels considering the data in Ref. 28, 27, 24. The derived half-life lower limits for these decays have been reported in Table 2. In particular, the half-life lower limits for the transitions of $^{176}\mathrm{Hf} \rightarrow {}^{172}\mathrm{Yb}$ ($0^+ \rightarrow 0^+$) and $^{177}\mathrm{Hf} \rightarrow {}^{173}\mathrm{Yb}$ ($7/2^- \rightarrow 5/2^-$) are close to the theoretical predictions (see Table 2).

Except for the α decay of ^{174}Hf for the transition $0^+ \rightarrow 2^+$, all the other limits ($\sim 10^{14} - 10^{20}$ y) are very far from the theoretical predictions.

In Ref. 24, it has also been evaluated the average Q.F. for alpha particles modelled according to the prescription of Ref. 35 and reported in Fig. 6; it varies in

the range 0.3–0.4. Dedicated measurements with α sources and using calibrated absorbers, possibly in vacuum, would be interesting to better study the Q.F.

Finally, the CHC crystal scintillator of Ref. 24 exhibits a very interesting PSD capability as shown in Fig. 5 and a Th/U residual contamination of few mBq/kg.

References

1. P. Belli *et al.*, *Particles* **4**(2) (2021) 241–274.
2. P. Belli *et al.*, *Universe* **6**(12) (2020) 239.
3. K. Blaum *et al.*, *Rev. Mod. Phys.* **92** (2020) 045007.
4. P. Belli *et al.*, *Eur. Phys. J. A* **55**(8) (2019) 140.
5. P. Belli *et al.*, *Eur. Phys. J. A* **50** (2014).
6. A. S. Barabash *et al.*, *Nucl. Instrum. Meth. A* **833** (2016) 77–81.
7. F. A. Danevich *et al.*, *AIP Conf. Proc.* **1549**(1) (2013) 201–204.
8. A. S. Barabash *et al.*, *Phys. Rev. D* **98**(9) (2018) 092007.
9. P. Belli *et al.*, *Phys. Rev. C* **85** (2012) 044610.
10. P. Belli *et al.*, *Nucl. Instrum. Meth. A* **935** (2019) 89–94.
11. R. Bernabei *et al.*, *AIP Conf. Proc.* **1549**(1) (2013) 189–196.
12. M. Barucci *et al.*, *Nucl. Instrum. Meth. A* **935** (2019) 150–155.
13. P. Belli *et al.*, *Nucl. Phys. A* **990** (2019) 64–78.
14. A. S. Barabash *et al.*, *Nucl. Phys. Atom. Energy* **19**(2) (2018) 95–102.
15. P. Belli *et al.*, *J. Phys. G* **45**(9) (2018) 095101.
16. A. S. Barabash *et al.*, *JINST* **15**(7) (2020) C07037.
17. P. Belli *et al.*, *Eur. Phys. J. A* **55**(11) (2019) 201.
18. P. Belli *et al.*, *Phys. Rev. C* **102**(2) (2020) 024605.
19. V. Caracciolo *et al. Nucl. Instrum. Meth. A* **901** (2018) 150–155.
20. O. Azzolini *et al.*, *Phys. Lett. B* **822** (2021) 136642.
21. P. Belli *et al.*, *Nucl. Phys. Atom. Energy* **19**(3) (2018) 220–226.
22. P. Belli *et al.*, *J. Phys. G* **48**(8) (2021) 085104.
23. M. Wang *et al.*, *Chin. Phys. C* **45** (2021) 030003.
24. V. Caracciolo *et al.*, *Nucl. Phys. A* **1002** (2020) 121941.
25. M. Mirea *et al.*, Rom. Rep. Phys. **67**(3) (2015) 872–889.
26. F. A. Danevich *et al. Nucl. Phys. A* **996** (2020) 121703.
27. B. Broerman *et al.*, *Nucl. Phys. A* **1012** (2021) 122212.
28. F. A. Danevich *et al. Eur. Phys. J. A* **56**(1) (2020).
29. J. Meija *et al.*, *Pure Appl. Chem.* **88** (2016) 293.
30. B. Buck *et al.*, *Phys. G* **17** (1991) 1223.
31. D. N. Poenaru and M. Ivascu *J. Physique* **44** (1983) 791.
32. V. Yu. Denisov *et al.*, *Rhys. Rev. C* **92** (2015) 014602.
33. A. Abzouzi *et al. J. Rad. and Nucl. Chem. Lett.* **135** (1998).
34. C. Cardenas *et al. Nucl. Instrum. Methods A* **869** (2017) 63.
35. V. I. Tretyak, *Astropart. Phys.* **33** (2010) 40.
36. R. D. Macfarlane and T. P. Kohman, *Phys. Rev.* **121** (1961) 1758.
37. A. Wald and J. Wolfowitz, *J Ann. Math. Stat.* **11** (1940) 147.